A&A 515, A101 (2010)
DOI: 10.1051/0004-6361/200913894

Astronomy & Astrophysics

Comparing six evolutionary population synthesis models by performing spectral synthesis for galaxies

X. Y. Chen[1,2,3], Y. C. Liang[1,2], F. Hammer[4], Ph. Prugniel[5], G. H. Zhong[1,2,3], M. Rodrigues[4], Y. H. Zhao[1,2], and H. Flores[4]

[1] National Astronomical Observatories, Chinese Academy of Sciences, A20 Datun Road, 100012 Beijing, PR China
e-mail: [chenxy;ycliang]@bao.ac.cn
[2] Key Laboratory of Optical Astronomy, NAOC, Chinese Academy of Sciences, PR China
[3] Graduate School of the Chinese Academy of Sciences, 100049 Beijing, PR China
[4] GEPI, Observatoire de Paris, CNRS-UMR 8111, 5 place Jules Janssen, 92195 Meudon, France
[5] Université Lyon 1, Villeurbanne, 69622 CRAL, Observatoire de Lyon, St Genis Laval, 69561 CNRS, UMR 5574, France

Received 17 December 2009 / Accepted 9 February 2010

ABSTRACT

Aims. We compare six popularly used evolutionary population synthesis (EPS) models by fitting the full optical spectra of six representative types of galaxies (star-forming and composite galaxies, Seyfert 2s, LINERs, E+A, and early-type galaxies) taken from the Sloan Digital Sky Survey (SDSS). We explore the dependence of stellar population synthesis results on the main ingredients of the EPS models and study whether there is an age sequence among these types of galaxies.
Methods. We use the simple stellar populations (SSPs) of each EPS model and the software STARLIGHT to perform our fits. Firstly, we explore the dependence of stellar population synthesis on EPS models by fixing the age, metallicity, and initial mass function (IMF) to construct a standard SSP group. We then use the standard SSP group of each EPS model (BC03, CB07, Ma05, GALEV, GRASIL, and Vazdekis/Miles) to fit the spectra of star-forming and E+A galaxies. Secondly, we fix the IMF and alter the age and metallicity to construct eight additional SSP groups. We then use these SSP groups to fit the spectra of star-forming and E+A galaxies to verify the effects of age and metallicity on stellar populations. Finally, we study the effect of stellar evolution tracks and stellar spectral libraries on our results, and present a possible age sequence among these types of galaxies.
Results. Using different EPS models, the numerical values of contributing light fractions obviously change, even though the dominant populations are unaltered. The stellar population synthesis does depend on the selection of age and metallicity, but does not depend significantly on the stellar evolution track. The importance of young populations decreases from star-forming, composite, Seyfert 2, LINER, to early-type galaxies, and the properties of E+A galaxies are between composite galaxies and Seyfert 2s in most cases.
Conclusions. Different EPS models infer different stellar population parameters, so that it is not reasonable to directly compare stellar populations estimated from different EPS models. To obtain reliable results, we should use the same EPS model to derive the parameter values that we compare.

Key words. galaxies: evolution – galaxies: Seyfert – galaxies: starburst – galaxies: stellar content – stars: evolution

1. Introduction

Stellar populations are fundamental components in studying the formation and evolution of galaxies. The formation of spiral galaxies remains hotly debated, and two main channels have been proposed, either initial collapse of gas at very high redshift in the framework of the tidal torque theory (Eggen et al. 1962; White 1984), or gaseous-rich mergers at intermediate to high redshifts (Hammer et al. 2005, 2007, 2009). These two channels of galaxy formation may produce distinctive stellar population properties, and it is relevant to test whether or not stellar population models can be used to identify these differences (see for example Heavens et al. 2004; Panter et al. 2007). Stars cannot be resolved for the majority of galaxies, and we therefore depend on models developed to analyze stellar populations by the study of the integrated light of galaxies, which holds information about the age and metallicity distributions of their stellar populations and star formation histories. This is the so-called stellar population synthesis on galaxies. Two main types of approaches have been developed: the empirical population synthesis (Faber 1972; Bica 1988; Boisson et al. 2000; Cid Fernandes et al. 2001) and the EPS (Tinsley 1978; Bruzual 1983; Worthey 1994; Leitherer & Heckman 1995; Maraston 1998; Vazdekis & Arimoto 1999; Bruzual & Charlot 2003; Maraston 2005; Cid Fernandes et al. 2005). In the empirical population synthesis approach, also known as "*stellar population synthesis with a database*", the observed spectrum of a galaxy is reproduced by a combination of spectra of individual stars or star clusters with different ages and metallicities from a library. The results following this approach do not consider the stellar evolution, and do not allow one to predict the past and future spectral appearance of galaxies.

The EPS approach uses the knowledge of stellar evolution to model the spectrophotometric properties of stellar populations, and has enjoyed more widespread use. In this approach, the main adjustable parameters are the stellar evolution tracks, the stellar spectral library, the IMF, the star formation history (SFH), and the grids of ages and metallicities. EPS represents a real physical model but is restricted by the lack of comprehensive stellar spectral library, accurate IMF and SFH, and poor understanding of some advanced phases of stellar evolution, such as the blue

stragglers (BSs), the horizontal branch (HB) stars, and the thermally pulsating asymptotic giant branch (TP-AGB) stars.

Up to now, several EPS models have been proposed and widely used in the stellar population studies of galaxies by analyzing their colors, spectra and multiwavelength spectral energy distributions (SEDs), such as BC93 (Bruzual & Charlot 1993), Pégase (Fioc & Rocca-Volmerange 1997), GRASIL (Silva et al. 1998), GALAXEV (Bruzual & Charlot 2003, BC03), CB07 (Charlot & Bruzual 2009, in preparation), SPEED (Jimenez et al. 2004), BaSTI (Pietrinferni et al. 2004; Cordier et al. 2007), Ma05 (Maraston 2005), Starburst 99 (Vázquez & Leitherer 2005), Vazdekis/Miles (Sánchez-Blázquez et al. 2006; Vazdekis et al., in preparation), GALEV (Anders & Alvensleben 2003; Kotulla et al. 2009), SPoT (Raimondo et al. 2005). Some studies have used these EPS models to analyze the stellar populations in galaxies and star clusters, and even compared them. The results are interesting, however, most of them focusing on analyzing the colors and multiwavelength SEDs of the systems.

Maraston et al. (2006) used two sets of EPS models to estimate the star formation histories, ages, and masses of seven galaxies in the Hubble Ultra Deep Field by analyzing their observed Spitzer mid-IR (the rest-frame-UV) photometry data. One of the EPS models chosen was Ma05, which includes the contribution of TP-AGB stars, and the other was BC03 (similar models are e.g., Pégase, Starburst 99). When they assumed zero reddening they concluded that Ma05 provided more accurate fits than BC03 to the data of these distant passively evolving galaxies at $1.4 < z < 2.7$. After dust was included in the fits, Ma05 performed no better than BC03. Lee et al. (2007) reconstructed some composite grids by using BC03, Ma05, and SPoT in the color-color diagrams to estimate the average age and metallicity of spiral galaxies. They found that the scatter for the various models was large at ages <2 Gyr, the dominant uncertainties being related to the treatment of different evolutionary phases (e.g., convective core overshoot, TP-AGB, helium abundance at higher metallicities). Longhetti & Saracco (2009) found that using different models (BC03, Ma05, Pégase, and GRASIL) did not significantly change the stellar mass estimates of early-type galaxies. Their samples were 10 massive early-type galaxies at $1 < z < 2$. Muzzin et al. (2009) fit the UV to NIR SEDs of 34 K-selected galaxies at $z \sim 2.3$ (Kriek et al. 2006, 2007, 2008) by using BC03, Ma05, and CB07. They concluded that no model was superior to any other. Carter et al. (2009) reproduced the optical and near-infrared colors of 14 nearby elliptical and S0 galaxies by using seven different EPS models (BC03; Pégase; Starburst 99; GALEV; SPEED; Ma05; BaSTI). Their results showed broad agreement between the ages and metallicities derived from different EPS models, although a wide range of significant deviations from the measured broad-band fluxes were found for the models.

Conroy et al. (2009, 2010) and Conroy & Gunn (2010) studied the propagation of uncertainties in stellar population synthesis modeling. In their first work, they explored the relevance of uncertainties in stellar evolution, IMF, and stellar metallicity distributions to the derived physical properties. They subsequently investigated some of the uncertainties associated with translating synthetic galaxies into observables, such as stellar evolution and dust. In their third work, they performed in particular the model calibration, comparison, and evaluation, and the models included their own flexible stellar population synthesis model (FSPS), BC03, and Ma05. They found that the FSPS and BC03 models were able to reproduce the optical and near-IR colors of E+A galaxies, while the Ma05 model performed poorly. They also pointed out significant differences between Ma05, BC03, and FSPS in terms of the photometry of intermediate-age and subsolar metallicity star clusters (i.e., star clusters in the MCs). In particular, the performance of their FSPS was superior to BC03 and Ma05 in these cases.

Some other works have also been applied to star clusters. Hempel et al. (2005) presented the results of optical and near-infrared photometry for globular cluster systems of two giant ellipticals. They compared the $(V - H)$ and $(V - I)$ colors predicted by BC03 and Ma05, and found the color predictions for a given age did not differ significantly, except for metal-poor objects of age $\leqslant$2 Gyr. Pessev et al. (2008) adopted 54 star clusters to evaluate the performance of four EPS models (Vazdekis 1999, BC03, Ma05, GALEV) in optical/near-infrared colour-colour space. They argued that each model had strong and weak points, and that no model was distinctive in all aspects.

There have also been some analyses more generally of the spectra of galaxies or star clusters. For example, Panter et al. (2007) used MOPED to study the star formation history, the stellar mass function, and the current stellar mass density of a large sample of SDSS DR3 galaxies. They also investigated the effects of the choices of the spectral resolution, sky lines, IMF, and EPS models (SPEED, Pégase, BC93, Ma05, BC03, CB07) on these properties. Their conclusion was that the main uncertainties in the estimate of the SFH were caused by the EPS model, the calibration of the observed spectra, and the choice of IMF. They subsequently investigated the impact of model choices by recovering the metallicity history using the same six EPS models, and suggested that older EPS models did not produce clear results (Panter et al. 2008). Cid Fernandes and his colleagues have studied the spectral synthesis on the SDSS galaxies by using the BC03 model and their STARLIGHT code. They also measured the properties of the galaxies, such as the dust extinction, stellar mass, SFH (Cid Fernandes et al. 2004, 2005, 2007; Mateus et al. 2006; Asari et al. 2007, 2009; Stasińska et al. 2008). Koleva et al. (2008) compared different models, and found that the Pégase-HR (Le Borgne et al. 2004) and Vazdekis/Miles models were in precise agreement, while the BC03 model exhibited biases, which might be due to the poor metallicity coverage of STELIB library causing unreliable results at non-solar metallicities. In Koleva et al. (2009a), they used full-spectrum fitting to derive the radial profiles of the SSP-equivalent ages and metallicities for a sample of 16 dwarf elliptical galaxies with their VLT spectra, and discussed the sensitivity of their results to the population model and IMF. Cid Fernandes & Gonzalez Delgado (2009) and Gonzalez Delgado & Cid Fernandes (2009) studied the ages, metallicities, and dust extinction of 27 star clusters in the Magellanic Clouds (from Leonardi & Rose 2003) by means of stellar population synthesis. They adopted STARLIGHT to fit their integrated optical spectra for the blue-near-UV range (3650–4600 Å), compared their results for different combinations of model and spectral library.

Despite this impressive progress in the accuracy of the stellar population analysis of galaxies and agreement between different EPS models, we can easily notice that most of them predict colors and multiwavelength SEDs of galaxies. There has been no similar analysis involving the fitting of the full spectra of galaxies, i.e., the detailed fittings of their stellar absorption lines and continua. Although some analyses have fitted spectra to study the properties of galaxies, there have been no similar efforts to compare the different EPS models by fitting spectra. Therefore, in this work, we compare six popularly used EPS models carefully by fitting the good quality optical spectra of a representative sample of galaxies taken from SDSS.

The SDSS provides high quality spectra of hundreds of thousands of galaxies and many other types of astronomical objects (such as AGNs) at medium resolution (3 Å, $R = 2000$) (Tremonti et al. 2004; Kauffmann et al. 2003; Brinchman et al. 2004). These data can be used to perform reliable stellar population analyses of representative samples of galaxies by means of full-spectrum fitting to continua and stellar absorption lines. It also provides a good way to compare the different EPS models.

In this work, we compare six different EPS models (BC03, CB07, Ma05, GALEV, GRASIL, and Vazdekis/Miles), by performing a spectral synthesis analysis of six representative types of galaxies from SDSS: 419 star-forming, 326 composite galaxies, 35 Seyfert 2s, 69 LINERs, 502 E+A galaxies, and 754 early-type galaxies. Hence, we check the dependences of the main ingredients of EPS models, i.e., the ages, metallicities, and stellar evolution tracks, on the stellar population analysis results.

We attempt to answer the following questions. Do these different EPS models (with similar ingredients) infer similar stellar population properties for a given galaxy? If there are differences, which of the main ingredient has the strongest influence? Do the stellar populations of these representative galaxies exhibit any age sequence among them? This final question is interesting and important, although our main aim is to check for consistency between the models using a single program.

This paper is organized as follows. In Sect. 2, the detailed illustration about the six EPS models and their main ingredients are performed. The sample selections are given in Sect. 3. In Sect. 4, we present the methods and the spectral synthesis results of different EPS models, and then compare these models. The dependences of ages and metallicities on the stellar populations of galaxies are also checked. In Sect. 5, we discuss the dependences of stellar populations of galaxies on stellar evolution tracks, and present a possible age sequence for the different types of galaxies. Summary and conclusions are given in Sect. 6. Throughout this paper, we assume the cosmological parameters $\Omega_{\rm M} = 0.3$, $\Omega_\Lambda = 0.7$, and $H_0 = 70\ {\rm km\,s^{-1}\,Mpc^{-1}}$.

2. EPS models

We present the six EPS models that we use and compare in our stellar population analysis of galaxies. They are BC03, CB07, Ma05, GALEV, GRASIL, and Vazdekis/Miles. Their main ingredients are stellar evolutionary tracks, a stellar library, grids of ages and metallicities, an IMF, and the SFH.

2.1. The main ingredients of an EPS model

One of the principal ingredients of an EPS model is the stellar evolutionary track, which records the evolution of stars of any mass from the zero-age main sequence to later evolutionary stages. Tracks covering a wide range of mass and time are necessary for EPS, and many groups have produced publicly available stellar evolutionary models: Padova 1994 (Pa 94; Alongi et al. 1993; Bressan et al. 1993; Fagotto et al. 1994a,b; Girardi et al. 1996) includes all phases of stellar evolution from zero-age main sequence to the beginning of TP-AGB (for low- and intermediate- mass stars) and core-carbon ignition (for massive stars); Padova 1999 (Pa 99) extends earlier models by the inclusion of the TP-AGB phase for stars in the mass range $2\ M_\odot \leqslant m \leqslant 7\ M_\odot$ in accordance with the fuel consumption theorem (Schulz 2002); Padova 2000 (Pa 00; Girardi et al. 2000); Geneva (Schaller et al. 1992); Cassisi (Cassisi et al. 1997a,b, 2000); and Marigo & Girardi (2007), which is a new synthetic model of the TP-AGB evolution.

The stellar spectral library is another important ingredient of the EPS model. An ideal stellar library should provide complete coverage of the HR diagram, accurate atmospheric parameters (e.g., $T_{\rm eff}$, surface gravities log g, metallicities Z), good wavelength coverage, high spectral resolution and robust calibration. Bruzual (2005) and Coelho (2009) reviewed some characteristics of different stellar spectral libraries. There are two types of stellar spectral libraries: an empirical library and a theoretical library. The empirical library (e.g., STELIB, Le Borgne et al. 2003; UVES POP, Valdes et al. 2004; Indo-US, Jehin et al. 2005; MILES, Sánchez-Blázquez et al. 2006; ELODIE, Prugniel et al. 2007) is based on the observations of real stars, so that it is more reliable. However, it is limited by the quality of the observations, thus the coverage of parameters are biased towards the typical stellar population targeted by the observations. The theoretical spectral library (e.g., Kurucz 1992; BaSeL 1.0, Lejeune et al. 1997, 1998) is based on model atmospheres, so that its coverage of parameters can be as comprehensive as necessary, but limited by our knowledge of the physics of stellar atmospheres.

The third important ingredient in EPS model is the IMF, i.e., the initial distribution of the stars along the main sequence. Pioneered by Salpeter (1955), many types of IMF have emerged (e.g., Kennicutt 1983; Scalo 1998; Kroupa 2001; Chabrier 2003). The general form of the IMF is $\phi(M) \propto M^{-(1+\alpha)}$, and the logarithmic slope and the upper and lower limits of the IMF are particular relevant to EPS.

With the above three main ingredients (stellar evolution track, stellar spectral library, and the IMF), we can construct SSPs. The time-dependent SSPs can then be convolved with an arbitrary SFH to predict the spectrum or colors of a galaxy (Kennicutt 1998). Throughout this work, we assume an instantaneous burst SFH, i.e., that $\psi(t) = 1\ M_\odot\ \delta(t)$.

2.2. BC 03

The popular library of evolutionary stellar population synthesis models GALAXEV is computed using the isochrone synthesis code BC03 (Bruzual & Charlot 2003). The SSP models given by BC03 span a wide range of wavelength (91 Å–160 μm, $N = 6900$), age (0–20 Gyr, $N = 221$), and metallicity Z (0.0001–0.05, $N = 6$). These models mainly use the STELIB/BaSeL3.1 libraries (Le Borgne et al. 2003; Lejeune et al. 1997, 1998; Westera et al. 2002, and references therein) with resolutions of 3 Å (*FWHM*) from 3200 Å to 9500 Å, and 20 Å (*FWHM*) elsewhere. In addition, BC03 provides models that rely on STELIB/Pickles libraries (Pickles 1998). There are 2 IMFs (Chabrier, Salpeter) and 3 stellar evolutionary tracks (Pa 94, Pa 00, and Geneva) that we can choose. This information is presented in Table 1.

2.3. CB 07

CB07 is a new version of BC03, which includes the new stellar evolution prescription of Marigo & Girardi (2007) for the TP-AGB evolution of low- and intermediate-mass stars. It is presented in Charlot & Bruzual (2009, in preparation), and we have obtained the model by private communication. The SSP models given by the current version of CB07 span a range of wavelengths (91 Å–36000 μm, $N = 6917$), age (0–20 Gyr, $N = 221$), and Z(0.0001–0.05, $N = 6$). There are also two choices of IMF, Chabrier and Salpeter. This information is shown in Table 1.

Table 1. Comparison of parameters in each EPS model.

Models	BC03	CB07	Ma05	GALEV	GRASIL	Vazdekis/Miles
library	STELIB/BaSeL3.1	STELIB/Kurucz92	BaSeL2.0	BaSeL2.0	Kurucz 1992	Miles 2006
resolution (Å)[a]	3	3	20	20	20	2.3
wavelength (Å)	91–1.6×10^6	91–3.6×10^8	91–1.6×10^6	91–1.6×10^6	91–1.2×10^7	3540–7410
N_λ	6900	6917	1221	1221	1264	4300
age (Gyr) (Number)	0–20(221)	0–20(221)	10^{-6}–15(67)	4×10^{-3}–16(4000)	10^{-4}–20(55)	0.06–18(50)
Z (Number)	0.0001–0.05(6)	0.0001–0.05(6)	0.0001–0.07(6)	0.0004–0.05(5)	0.0001–0.1(7)	0.0001–0.03(7)
IMF	Salpeter	Salpeter	Salpeter	Salpeter	Salpeter	Salpeter
track	Pa 94	Pa 94+Marigo 07	Cassisi+Geneva	Pa 99	Pa[b]	Pa 00

Notes. [(a)] Resolution in visual regions. [(b)] Refer to Bertelli et al. (1994).

2.4. Ma05

The original version of Ma05 is Ma 98, which is an EPS model based on the fuel consumption theorem, in contrast to the other models that consists of a grid of SSP models with $Z = Z_\odot$ and an age range of 30 Myr–15 Gyr. Ma 05 spans a wider range of stellar population parameters: 6 metallicities ($Z = 0.0001$–0.07), 67 ages (10^3 yr–15 Gyr), 2 IMFs (Salpeter, Kroupa), and 3 horizontal branch (HB) morphologies (red, intermediate or blue; see details in Maraston 2005). However, for each metallicity, predictions are not available for all 67 ages: $Z = 0.0001$ associated with 16 ages (1–15 Gyr) with Cassisi tracks; $Z = 0.07$ associated with 16 ages (1–15 Gyr) with Pa 00 tracks; and the remaining 4 metallicities associated with the full 67 ages with Cassisi + Geneva tracks. The Cassisi tracks do not consider overshooting, while the Padova tracks include the effects of overshooting. The stellar spectra were taken from the BaSel library (Lejeune et al. 1998), of low spectral resolution, i.e., 5–10 Å as red as the visual region, and 20–100 Å in the near-IR (wavelength ranges from 91 Å to 160 μm, and $N_\lambda = 1221$). This information is given in Table 1.

2.5. GALEV

GALEV (GALaxy EVolution) evolutionary synthesis models describe the spectral and chemical evolution of galaxies over cosmological timescales, i.e., from the beginning of star formation to the present (Kotulla et al. 2009). This code considers both the chemical evolution of the gas and the spectral evolution of the stellar component, allowing for what they call a chemically consistent treatment. Thus, some SSPs in this model exhibit emission lines in their spectra. The GALEV evolutionary synthesis models are available via a web-interface[1]. The SSP models provided by this code cover 5 metallicities ($0.02 \leqslant Z/Z_\odot \leqslant 2.5$), and 4000 ages ($4 \times 10^6$ yr–16 Gyr) in time-steps of 4 Myr. They are based on spectra from Lejeune et al. (1997, 1998) (BaSeL 2.0) for 3 IMFs (Salpeter, Scalo, and Kroupa), and on the theoretical isochrones from the Pa 99 and the Geneva tracks. The lower limit to the stellar mass for the IMF is always 0.1 $M_\odot$, while the upper mass limits are as follows: for Padova, it is limited by isochrones (about 50 $M_\odot$ for super-solar metallicity and about 70 $M_\odot$ for the remainder); for Geneva, it is always 120 $M_\odot$. The range of wavelength is 90 Å–160 μm with resolution of 20 Å in the UV-optical and 50–100 Å in the NIR ranges (Schulz et al. 2002; Anders & Alvensleben 2003). This information is given in Table 1.

2.6. GRASIL

GRASIL (GRAphite and SILicate) is a population synthesis code, which takes into full account the effects of the dusty interstellar medium on galaxy spectra (Silva et al. 1998). It is a multiwavelength model for the combination of stellar population and dust, which absorbs and scatters optical and UV photons and emits in the IR-submm region. It is particularly suited to the study of the IR properties of dusty galaxies. In addition, GRASIL can be very conveniently operated using the web interface GALSYNTH[2]. The SSP models given by this code spans a wide range of metallicity ($Z = 0.0001$–0.1, $N = 7$) and age (10^5 yr–20 Gyr, $N = 55$). The models are based on the Kurucz (1992) stellar atmosphere model, on 4 IMFs (Salpeter, Kennicutt 1983, Miller & Scalo and Scalo) with mass ranges 0.15–120 $M_\odot$, and on the Padova tracks (Bertelli et al. 1994), which account adding for the effects of dusty envelopes around AGB stars (see details in Silva's Ph.D. thesis). The spectra range from 91 Å to 1200 μm with resolution of 20 Å. This information is given in Table 1.

2.7. Vazdekis/Miles

The EPS model explored by Vazdekis et al. was developed in 1996, experienced several revisions, and predictions for old and intermediate age stellar populations. The original version V96 (Vazdekis et al. 1996) adopted the Lick polynomial fitting functions based on the Lick/IDS stellar library, although with the caveat that the Lick stellar library had not been flux calibrated (V96). Vazdekis then extended V96 to provide flux-calibrated spectra (Vazdekis 1999, V99). This version (V99) predicted SEDs for SSPs in two restricted spectral regions in the optical wavelength range (3855–4476 Å, 4795–5465 Å) at resolution ~1.8 Å (*FWHM*) with a range of Z ($-0.7 \leqslant \log(Z/Z_\odot) \leqslant +0.2$) and ages (1 to 17 Gyr). The input stellar database is the empirical stellar library of Jones (1999). Four types of IMFs are considered in this version: unimodal, bimodal, Kroupa universal, and Kroupa revised (Vazdekis et al. 2003, and references therein). A revised version of the model of V96 and V99 was also presented (Vazdekis et al. 2003), which replaced the database of Jones (1999) with Cenarro (2001), and replaced the isochrones of Bertelli (1994) with Pa 00. This model predicted both the strength of the Ca II triplet feature and SEDs in the range 8449–8952 Å at resolution 1.5 Å (*FWHM*), with metallicities $-1.7 < [\mathrm{Fe/H}] < +0.2$, ages 0.1–18 Gyr, and 4 types of IMFs (as in V99). In this code, we adopted the latest version

[1] http://www.galev.org

[2] http://galsynth.oapd.inaf.it/galsynth/index.php

based on a new empirical stellar spectral library MILES (Sánchez-Blázquez et al. 2006). The model covers the wavelength range 3540–7410 Å at resolution ~2.3 Å (*FWHM*), 7 metallicities $-2.32 \leqslant \log(Z/Z_{\odot}) \leqslant +0.22$ with Pa 00 tracks, and 50 ages across the range 0.063–17.78 Gyr (Vazdekis et al., in preparation). This information is given in Table 1.

We summarize the related parameters of all the six EPS models in Table 1, which are the most frequent choices in stellar population analyse and used in this work.

3. Galaxy sample

We decided to study representative samples of six types of galaxies. These are 849 emission-line galaxies including 419 star-forming galaxies, 326 composite galaxies, 35 Seyfert 2s, and 69 LINERs (taken from Chen et al. 2009), in addition to both 502 E+A galaxies (from Goto 2007) and 754 early-type galaxies (from Hao et al. 2006). We obtained all the 1D spectra from the SDSS database, which had been sky-subtracted and had their telluric absorption bands removed, prior to being wavelength and spectrophotometrically calibrated (Stoughton et al. 2002). We corrected the foreground Galactic extinction using the reddening maps of Schlegel et al. (1998) and then shifted the spectra into the rest frame. To measure the global properties of the galaxies in each of the subgroups, we combined all spectra in each of the subgroups using the task SCOMBINE in IRAF[3], that is, we combined spectra by interpolating them to a common dispersion sampling, and computing the median intensity of all pixels. In this way, we can also improve the *S/N* of the spectra typically between 26 and 56 in the 4730–4780 Å. Then we analyze these six combined spectra.

3.1. Emission-line galaxies

The emission-line galaxies were taken directly from Chen et al. (2009). A sample was selected from the main galaxy sample of the Sloan Digital Sky Survey (SDSS) DR4 database and then cross-correlated with the IRAS Point Source Catalog (PSCz) (5″ matching radius). We then selected high signal-to-noise ratio (*S/N*) targets according to the criteria of *S/N* greater than 5σ for Hβ, Hα, [NII]λ6583, and *S/N* greater than 3σ for [OIII]λ5007. In addition, the objects without spectra of the center of galaxies, and those with problematic mask spectra were all removed from our sample (see details in Chen et al. 2009). Finally, 849 objects remained in our emission-line galaxy subsample. The observed-frame spectral wavelength range is 3800–9200 Å, and the resolution is 3 Å (*FWHM*).

These emission-line galaxies were then divided into 4 groups of 419 star-forming galaxies, 326 composite galaxies, 35 Seyfert 2s, and 69 LINERs, according to the emission-line diagnostic diagram (see Fig. 2 in Chen et al. 2009; Baldwin et al. 1981, BPT; Shuder et al. 1981; Veilleux & Osterbrock 1987; Kewley et al. 2001; Kauffmann et al. 2003). Composite galaxies refer to objects whose spectra contain significant contributions from both AGN and star formation (Brinchmann et al. 2004; Kewley et al. 2006; Chen et al. 2009). Most of them have redshift $z < 0.1$ due to the limitations of IRAS observations.

3.2. E+A galaxies

E+A galaxies are so-called because their spectra resemble a superimposition of those of elliptical galaxies and A-type stars. On the one hand, the principal characteristics of elliptical galaxies are not related to morphology (although most are elliptical in shape) but to the non-detection of ongoing star formation their spectra do not exhibit significant emission lines. On the other hand, their strong Balmer absorption lines are reminiscent of the properties of A-type stars. Therefore, E+A galaxies have been interpreted as post-starburst galaxies, that is, a galaxy that has experienced a recent starburst, but truncated it suddenly. Some works have been performed on this type of galaxies (Falkenberg et al. 2009a,b; Huang & Gu 2009; Pracy et al. 2009, and references therein).

We selected our sample of E+A galaxies from the catalogue of Goto (2007), which was based on the SDSS DR5 and an extended sample from Goto (2005) on DR2. There were 564 E+A galaxies in this catalogue, and the selection algorithm can be summarized as follows: they only used objects classified as galaxies, those not spectroscopically classified as a star, and with spectroscopic $S/N > 10$ per pixel to remove the pollution from nearby stars and star-forming regions; they then selected E+A galaxies as those satisfying the criteria of Hδ equivalent width (EW) > 4 Å[4], [OII] $EW > -2.5$ Å, and Hα $EW > -3.0$ Å; they excluded galaxies at $0.35 < z < 0.37$ because of the sky emission line at 5577 Å. From this catalogue, we discarded 62 E+A galaxies because they have problematic mask spectra. Thus our final sample of E+A galaxies contains 502 objects.

3.3. Early-type galaxies

Early-type galaxies remain the most widely studied objects, because of their relatively low dust extinction, gaseous interstellar medium, and little recent star formation (Vazdekis et al. 1996; Cid Fernandes et al. 2009, and references therein).

Our sample of early-type galaxies was taken from Hao et al. (2006), which was based on the SDSS DR4 photometric catalogue. These authors selected objects at redshifts lower than 0.05, with the velocity dispersions that cover a range from 200 km s^{-1} to 420 km s^{-1}, whose images were not saturated or located at the edge of the corrected frame; they excluded some objects that were unavailable from the SDSS DR4 Data Archive Server (DAS), and those with visible dust lanes. Then they visually examined all images to confirm that the target objects were E/S0 galaxies and that their images were unaffected by companion galaxies or bright stars. We also discarded 93 objects with problematic mask spectra, so that our final sample of early-type galaxies contains 754 objects.

4. Comparisons of the six EPS models based on spectral synthesis

4.1. Spectral synthesis method

We attempted to reproduce the spectral absorption lines and continua of the sample galaxy spectra to study their stellar populations by using the software STARLIGHT[5] (Cid Fernandes et al. 2005, 2007; Mateus et al. 2006; Asari et al. 2007; Chen et al. 2009). This is a program that fits an observed spectrum O_{λ} with a model M_{λ} that combines up to N_* SSPs with different ages and metallicities from different stellar population synthesis models. A Gaussian distribution centered on a velocity v_* and broadened by σ_* models the line-of-sight stellar motions. The fit is

[3] http://iraf.noao.edu/

[4] Absorption lines are defined to have a positive *EW*.

[5] http://www.starlight.ufsc.br

Table 2. Selections of ages and metallicities for SSPs from each model, which we use below.

Models	Ages (Gyr)												Metallicities ($Z_\odot$)		
	Young (<0.2 Gyr)				Intermediate (0.2–2 Gyr)				Old (>2 Gyr)						
	Y1	Y2	Y3	Y4	I1	I2	I3	I4	O1	O2	O3	O4	Z1	Z2	Z3
BC03, CB07	0.004	0.010	0.064	0.102	0.286	0.509	0.905	1.434	3.00	6.00	10.00	13.00	0.2	1.0	2.5
Ma05	0.004	0.010	0.065	0.100	0.300	0.500	0.900	1.500	3.00	6.00	10.00	13.00	0.5	1.0	2.0
GALEV	0.004	0.012	0.064	0.100	0.280	0.500	0.900	1.432	3.00	6.00	10.00	13.00	0.2	1.0	2.5
GRASIL	0.004	0.010	0.060	0.100	0.300	0.500	0.900	1.500	3.00	6.00	10.00	13.00	0.2	1.0	2.5
Vazdekis/Miles			0.063	0.100	0.280	0.500	0.890	1.410	3.16	6.31	10.00	12.59	0.2	1.0	1.5

Notes. BC03 and CB07 are shown in the same line. See more details in Sect. 4.2.

carried out with the Metropolis scheme (Cid Fernandes et al. 2001), which searches for the minimum $\chi^2 = \Sigma_\lambda[(O_\lambda - M_\lambda)\omega_\lambda]^2$, where the reciprocal of weight ω_λ^{-1} is the error in O_λ except for masked regions. Pixels that are more than 3σ away from the rms $O_\lambda - M_\lambda$ are given zero weight by the parameter "*clip*". The STARLIGHT group has carefully checked the reliability of this software by analyzing the "stellar populations" of fake galaxies made by known SSPs (see Fig. 4 of Cid Fernandes et al. 2005; and Fig. 1 in Cid Fernandes et al. 2004).

In our fitting, we used the reddening law of Calzetti et al. (1994, CAL hereafter). The wavelength range considered was between 3700 and 7400 Å. A power law representing the non-stellar component (Koski et al. 1978) $F_\nu \propto \nu^{-1.5}$ was added when we fitted the spectra of Seyfert 2s and LINERs. The mask regions were the same as Chen et al. (2009), which include the strong emissionlines and bad pixels. In addition, we did not consider different weights for different regions of the spectra, since we found that this did not affect our spectral synthesis results.

One of the most important output parameters of STARLIGHT when analyzing the stellar population is the population vector $\boldsymbol{x}$. The component x_j ($j = 1, ..., N_*$) represents the fractional contribution of the SSP with age t_j and metallicity Z_j to the model flux at the normalization wavelength $\lambda_0 = 4020$ Å. Another important parameter, the mass fraction μ_j, has a similar meaning.

4.2. SSP selections

As mentioned in Sect. 2, we selected 12 (or 10) representative ages and 3 metallicities for each EPS model to construct different SSP groups when performing our fits, and we list the details in Table 2. We arranged the ages of SSPs into 3 bins: young populations of age <0.2 Gyr, intermediate-age populations of age between 0.2 Gyr and 2 Gyr, and old ones of age >2 Gyr. We note that these criteria are different from those of Chen et al. (2009), which followed the work of Kong et al. (2003) (i.e., young with age <0.58 Gyr, old with age >10 Gyr, and intermediate with ages between these two). The width of a Balmer absorption line is indicative of the age of a young population of age <1 Gyr, while the ones older than 1.5–2 Gyr are dominated by emission lines. From SDSS spectra, it is generally difficult to differentiate 3–5 Gyr populations from 10 Gyr populations, and Mathis et al. (2006) also pointed out that the signatures of intermediate-age stars (0.5–4 Gyr) are masked by those of both younger and older stars, so we adopt this new criteria here.

The logic of our work is in five steps as follows:

1. First, we fix some main ingredients for the EPS models, i.e., the stellar library, the stellar evolution track, and the IMF (Salpeter) are selected according to Table 1. An instantaneous burst SFH is always assumed.
2. We then select the first SSP group including 6 SSPs of at different ages and of solar metallicity (see Table 2) from each EPS model. It is called group **No. (1)** and is our "standard case" (see Table 3): two young SSPs ($Y1 = 0.004$, $Y2 \sim 0.01$ Gyr, except for Vazdekis/Miles, in which the youngest ages $Y3 \sim 0.06$ and $Y4 \sim 0.10$ Gyr are selected), two intermediate SSPs ($I2 \sim 0.5$, $I3 \sim 0.9$ Gyr), and two old SSPs ($O3 \sim 10$, $O4 \sim 13$ Gyr). This "standard case" will be used to analyze the stellar populations of star-forming and E+A galaxies in Sect. 4.3.
3. Next, we construct another three SSP groups by adding/removing some young, intermediate, and old SSPs of solar metallicity. We may then verify the age dependences. The corresponding three groups are:
   No. (2): 3 SSPs with ages of Y1 (Y3 for Vazdekis/Miles), I2, and O3 at $Z_\odot$ (Z2);
   No. (3): 9 (or 8) SSPs with ages of Y1, Y2, Y3, I2, I3, I4, O2, O3, O4 (only Y3 and Y4 for the young populations in Vazdekis/Miles);
   No. (4): 12 (or 10) SSPs with ages of Y1, Y2, Y3, Y4, I1, I2, I3, I4, O1, O2, O3, O4 (only Y3 and Y4 for the young populations in Vazdekis/Miles).
4. After that, we construct another three SSP groups by adding SSPs with sub-solar metallicity or/and super-solar metallicity based on group No. (1). We then verify the metallicity dependences. These three groups are:
   No. (5): 12 SSPs with 6 ages in common with the group No. (1) but at two metallicities: Z1 (0.2 or 0.5 $Z_\odot$) and Z2 ($Z_\odot$);
   No. (6): 12 SSPs with 6 ages as in group No. (1) but at two metallicities: Z2 ($Z_\odot$) and Z3 (2.0, 2.5 or 1.5 $Z_\odot$);
   No. (7): 18 SSPs with 6 ages as in group No. (1) but at three metallicities: Z1, Z2, and Z3.
5. We finally fix the ages and only change the metallicity of group No. (1) to build the last two SSP groups, to be able to check whether a age-metallicity degeneracy exists.
   No. (8): 6 SSPs with 6 ages as in group No. (1) but at sub-solar metallicity (Z1);
   No. (9): 6 SSPs with 6 ages as in group No. (1) but at super-solar metallicity (Z3).
   Table 3 list details of the 9 SSP groups Nos. (1)–(9).

4.3. Spectral analysis and comparisons among six different EPS models

Among the six EPS models, the SSPs of three of them (BC03, CB07, Vazdekis/Miles) are of similar spectral resolution, and are comparable to the resolution of SDSS spectra; another three (Ma05, GALEV, GRASIL) are of lower spectral resolution SSPs, ~20 Å. Thus, when we use SSPs in the latter three

Table 3. Seven SSP groups used in our stellar population analysis.

Models	SSPs	Ages	Metallicities	Notes
No. (1)	6 SSPs	Y1 Y2; I2 I3; O3 O4	Z2	
		Y3 Y4; I2 I3; O3 O4	Z2	for VM
No. (2)	3 SSPs	Y1; I2; O3	Z2	
		Y3; I2; O3	Z2	for VM
No. (3)	9 SSPs	Y1 Y2 Y3; I2 I3 I4; O2 O3 O4	Z2	
	8 SSPs	Y3 Y4; I2 I3 I4; O2 O3 O4	Z2	for VM
No. (4)	12 SSPs	Y1 Y2 Y3 Y4; I1 I2 I3 I4; O1 O2 O3 O4	Z2	
	10 SSPs	Y3 Y4; I1 I2 I3 I4; O1 O2 O3 O4	Z2	for VM
No. (5)	12 (6 × 2) SSPs	Y1 Y2; I2 I3; O3 O4	Z2 Z1	
		Y3 Y4; I2 I3; O3 O4	Z2 Z1	for VM
No. (6)	12 (6 × 2) SSPs	Y1 Y2; I2 I3; O3 O4	Z2 Z3	
		Y3 Y4; I2 I3; O3 O4	Z2 Z3	for VM
No. (7)	18 (6 × 3) SSPs	Y1 Y2; I2 I3; O3 O4	Z1 Z2 Z3	
		Y3 Y4; I2 I3; O3 O4	Z1 Z2 Z3	for VM
No. (8)	6 SSPs	Y1 Y2; I2 I3; O3 O4	Z1	
		Y3 Y4; I2 I3; O3 O4	Z1	for VM
No. (9)	6 SSPs	Y1 Y2; I2 I3; O3 O4	Z3	
		Y3 Y4; I2 I3; O3 O4	Z3	for VM

Notes. Please see Table 2 for the meanings of the symbols. "VM" refers to the model Vazdekis/Miles. Group No. (1) is our "standard case".

EPS models, we need to decrease the resolutions of the observed spectra to match those of the models. We attempted three ways of achieving this, first using the GAUSS task in IRAF, second using the Disgal1D algorithm developed by our French collaborators, and the third is the re-bin program kindly provided by Dr. Jingkun Zhao at NAOC. We found that there was no significant difference between the results for these three methods. Therefore, we finally adopted the GAUSS task in IRAF to reduce the resolution of our spectra.

In this section, we adopt SSP group No. (1) from 6 different EPS models to analysis the stellar populations. In this way, the age, metallicity, and IMF are all fixed, and the only variable is the EPS models, and we can check the dependence of stellar population synthesis on EPS models. We consider star-forming and E+A galaxies as examples, and analyze their stellar populations by using group No. (1) from these six EPS models, and compare our results.

4.3.1. Star-forming galaxies

In Fig. 1, we present the spectral fitting results and the light fraction distributions for the combined spectra of star-forming galaxies by using six SSPs (group No. (1) in Table 3) from six different EPS models. Every three panels as a group correspond to the results of one EPS model. The top panel shows the observed spectra (black line), the synthesis spectra (red line), and the error spectra (green line), the middle panel shows the residual spectra, and the bottom panel shows the light fraction distribution. From the top two panels in each model, we can see that the synthesis spectra reproduce the observed spectra well in most cases. However, we note that there is a trough around Hβ when we use BC03 and CB07, which disappears when we use Ma05, GALEV, GRASIL, and Vazdekis/Miles. Asari et al. (2007) suggested that this could relate to calibrations in the STELIB library in this spectral range, and we also confirmed this in our earlier work (Chen et al. 2009) by using star clusters. We speculate that the poor fit may also be caused by the way in which the continuum shape is fitted by Starlight. To check this point, we used yet another program, ULySS (Koleva et al. 2009b), to perform similar fits, and we achieved superior fits around Hβ. However, this problem does not significantly affect our stellar population analysis. Besides that, we find the Ma05, GALEV and GRASIL models seem to be superior in reproducing the important Balmer lines and continuum. This may due to the lower spectral resolution, which reduces the details in spectra.

The bottom panels in Fig. 1 show that the resultant stellar populations for different EPS models are not exactly the same for the star-forming galaxies, although the dominant populations are all young plus intermediate populations.

The top line of Table 4 presents the light fractions contributed by the young (Y), intermediate (I), and old (O) populations. The related numbers indicate that star-forming galaxies are composite young, intermediate, and old populations. The differences in the contributed light fractions of these EPS models are in the range 0.01–18.75%. Vazdekis/Miles differs from others, inferring 58% (27% more than that of CB07) young and 20% intermediate populations. The reason for this could be that Vazdekis/Miles has contains fewer data for young populations than the other models, and its youngest age is $Y3 = 0.063$ Gyr, older than others, which may explain the higher young population fraction that it infers. We believe that the errorbars of these inferred light fractions are small. Cid Fernandes et al. (2005) presented their errorbars centered on the mean values obtained by fitting 20 realizations of each of 65 test galaxies. Their three condensed populations are recovered well by Starlight, with uncertainties smaller than 0.05 (young: $t < 10^8$), 0.1 (intermediate: $10^8 < t < 10^9$), and 0.1 (old: $t > 10^9$) for $S/N \geqslant 10$. In our fittings, the code provides the values of last-chain-values for 7 chains, and we find that most of the discrepancies in these adopted values are less than 1%. We therefore do not consider errorbars in our studies here.

We also find that BC03 and CB07 infer a ~30% young stellar population and ~50% intermediate age one. All of Ma05, GALEV, and GRASIL infer comparable young and intermediate populations (both ~44% in Ma05) or a slightly higher young populations than the intermediate ones (~47% vs. 39% in GALEV; ~50% vs. 36% in GRASIL). In other words, there is an inversion of the dominant population between BC03, CB07 on the one side, and GALEV, GRASIL, and Vazdekis/Miles on the other side. To explain this phenomenon, we directly compare

Table 4. Stellar populations in star-forming and E+A galaxies by using different EPS models with SSP group No. (1) (Tables 2, 3).

Types	SSP groups	Age bin	BC03	CB07	Ma05	GALEV	GRASIL	Vazdekis/Miles
star-	No. (1)	Y	35	31	44	47	50	58
forming	6 SSPs	I	54	51	44	39	36	20
galaxies	$Z = Z2$	O	11	18	12	14	14	22
E+A	No. (1)	Y	13	9	13	22	20	19
galaxies	6 SSPs	I	77	75	79	71	70	65
	$Z = Z2$	O	10	15	8	7	10	16

Notes. Y represents young populations, I represents intermediate populations, and O represents old populations.

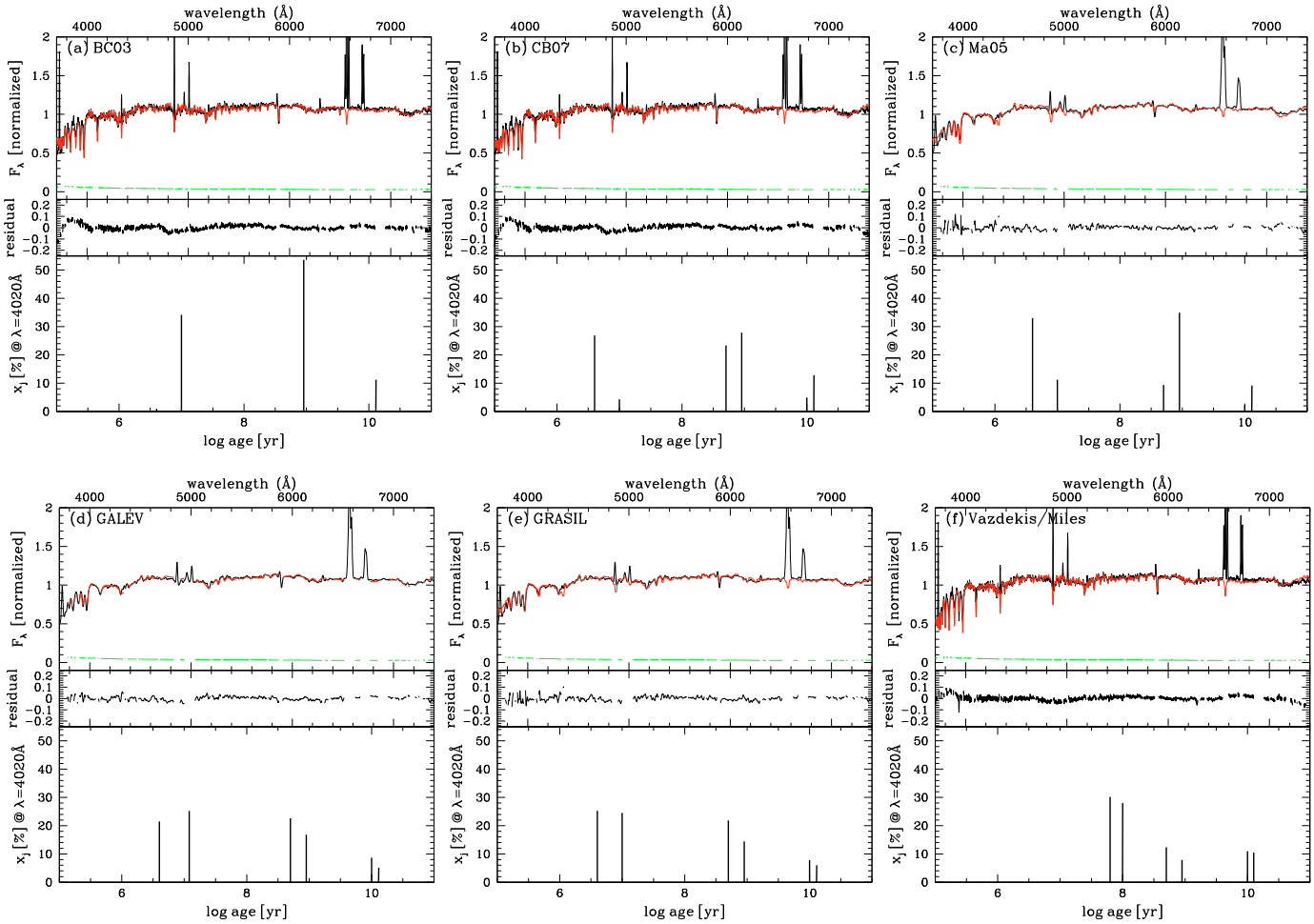

Fig. 1. Spectral fitting results of star-forming galaxies by using six SSPs (group No. (1)) from different models: **a)** BC03, **b)** CB07, **c)** Ma05, **d)** GALEV, **e)** GRASIL and **f)** Vazdekis/Miles. In each EPS model, *top panels*: comparison of synthesis spectrum (red line) with the observed spectrum (black line), and green line shows the error spectrum; *middle panels*: the residual spectrum; *bottom panels*: distributions of light fractions.

the 6 SSPs of these models that we used in the fittings, and find that the young SSPs of BC03 and CB07 have relatively higher fluxes at blue wavelengths than others when we normalize them at about 6000 Å. Considering Y2 as an example, GALEV and GRASIL represent one group, the fluxes at blue wavelengths of which are lower than for both BC03 and CB07, and Ma05 is in-between these two groups. This explains the inversion of young and intermediate populations between the two groups, and why Ma05 infers comparable young and intermediate fractions. As for Vazdekis/Miles, the two SSPs in the young age-bin are older than in the other bins, thus the fraction of the resulting young population is much higher than for the intermediate one. The reason for the difference in predictions of SSPs among these EPS models could be their different stellar libraries. STELIB is used by BC03 and CB07, but BaSeL2.0 or Kurucz are used in GALEV, Ma05, and GRASIL. The former is empirical based on real observed stellar spectra of higher resolution and the latter are theoretical of lower resolution. The limitations of the STELIB library were discussed by Koleva et al. (2008) and Gonzalez Delgado & Cid Fernandes (2009). Another possible reason for the differences between the two groups may be their spectral resolution, because BC03 and CB07 are of higher resolution (3 Å), while Ma05, GALEV and GRASIL are of lower resolution (20 Å). To check this, we degraded the 6 SSPs in BC03 from 3 Å to 20 Å, performed similar fits, and found that the discrepancies between the two groups had decreased.

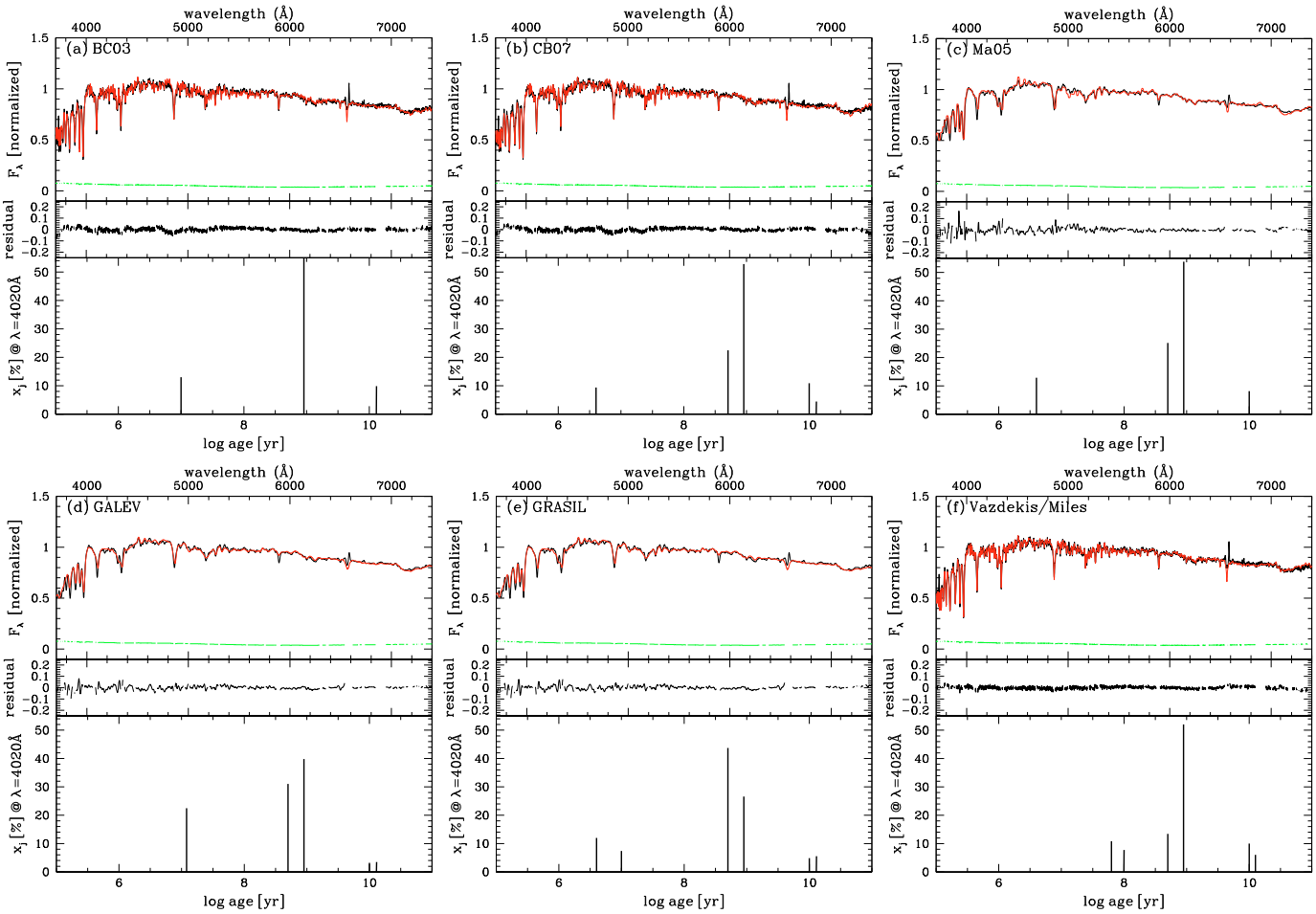

Fig. 2. Same as Fig. 1, but for E+A galaxies.

4.3.2. E+A galaxies

In Fig. 2, we present the spectral fitting results and the light fraction distributions of E+A galaxies derived by using six SSPs (group No. (1) in Table 3) from six different EPS models.

We found that the match between the synthesis spectra and the observed spectra is good. When considering BC03 and CB07, the troughs around H_β become shallower than that of star-forming galaxies, and disappear in panels corresponding to Ma05, GALEV, GRASIL, and Vazdekis/Miles, which confirm our conclusions for star-forming galaxies. The bottom panels of the figure also show that different EPS models do not predict exactly similar population properties for E+A galaxies, even though the peaks of the distributions are more concentrated.

In the bottom line of Table 4, we also list the implied light fractions of E+A galaxies. It shows that the contributions from different models vary within a range of 0.14–13.53%. The percentages of intermediate-age populations are all greater than 70% except for Vazdekis/Miles (65.45%). Thus we suggest that E+A galaxies are dominated by intermediate-age populations, and consist of young, intermediate-age and old populations.

We now summarize our results for the stellar population analyse of different EPS models as just presented, in which find that for different EPS models the numerical values of light fractions change obviously, although the dominant populations remain consistent. The EPS models also appear to have difficulties in distinguishing the stellar populations, i.e., for a given galaxy, different models infer a different order of importance for old, intermediate, and young stellar populations (especially in the case of star-forming galaxies). We suggest that the use of near-IR photometry may be a way of resolving this problem. However, as mentioned by Eminian et al. (2008), Maraston (2005), and Conroy et al. (2009), TP-AGB stars dominate the near-IR light of galaxies, and we should be aware that the uncertainties associated with the TP-AGB phase probably prevent significant improvements.

4.4. Dependences on ages and metallicities

We investigate the dependence of stellar population synthesis on the selection of age and metallicity. As mentioned in Sect. 4.2, and Tables 2, 3, we adopt nine SSP groups in total, Nos. (1)–(9).

4.4.1. Age dependences – SSP groups Nos. (2)–(4) in Table 3

As mentioned above, we fix the metallicity to be solar, then change only the selections of age to construct SSP groups Nos. (2)–(4). We then use SSP groups Nos. (2)–(4) from different EPS models to analyze the stellar populations of star-forming and E+A galaxies. The resulting stellar populations are compared with each other and also with group No. (1), so that we can check the age effects on our stellar population analysis.

The top panels in Fig. 3 show the light fractions of young (top-left panel), intermediate (top-middle panel), and old (top-right panel) populations for star-forming galaxies by using the

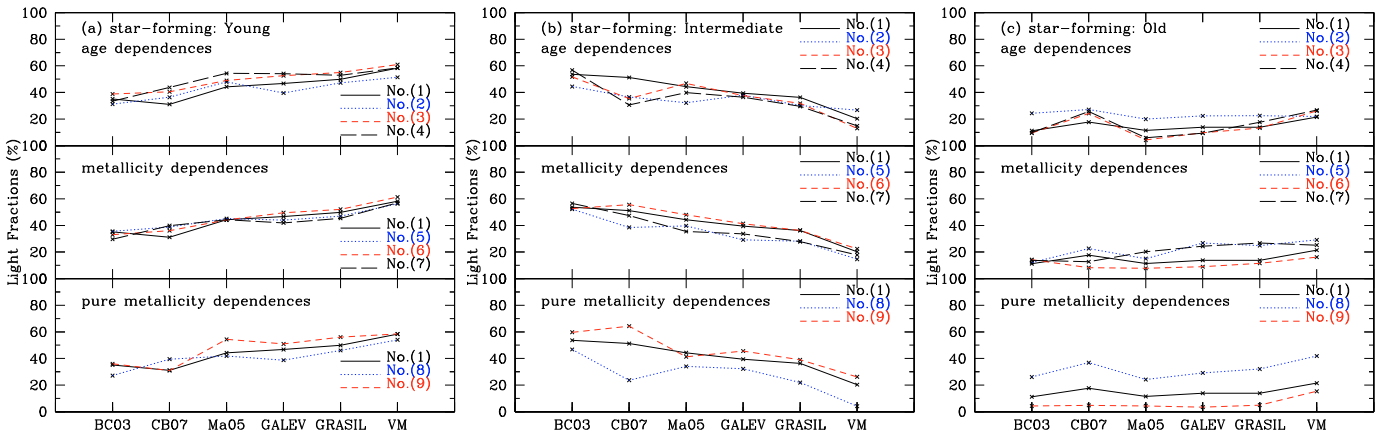

Fig. 3. The light fraction contributions to star-forming galaxies in bins of young population (*left three panels*), intermediate-age population (*middle three panels*), and old population (*right three panels*). The *x*-axis represents six EPS models, and the *y*-axis represents the light fractions in percentage. Different lines connect points from different SSP groups. *Top panels*: solid line stands for group No. (1), dotted line stands for group No. (2), short-dashed line stands for group No. (3), and long-dashed line stands for group No. (4). *Middle-panels*: solid line stands for group No. (1), dotted line stands for group No. (5), short-dashed line stands for group No. (6), and long-dashed line stands for group No. (7). *Bottom-panels*: solid line stands for group No. (1), dotted line stands for group No. (8), short-dashed line stands for group No. (9).

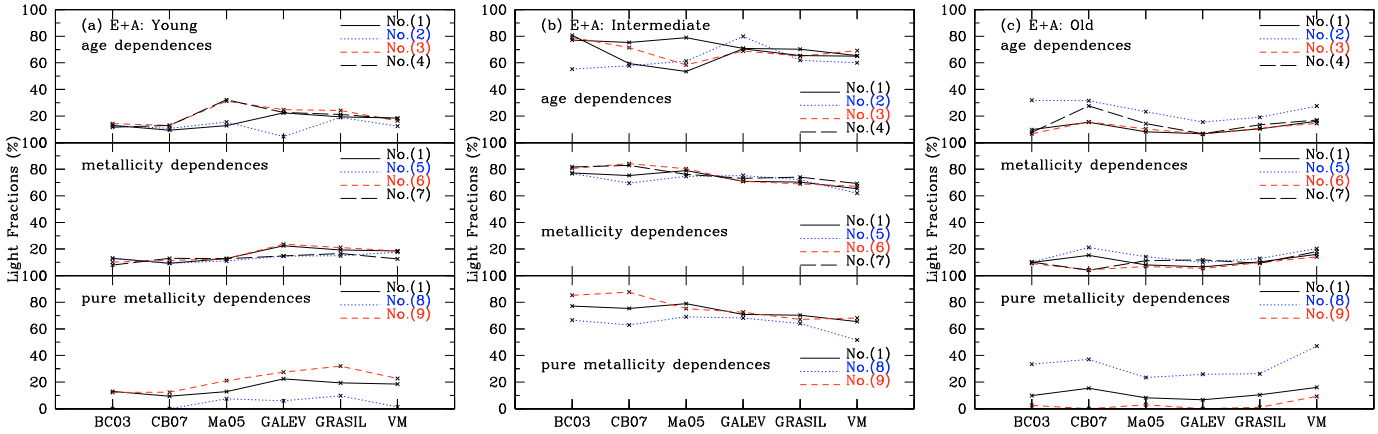

Fig. 4. Same as Fig. 3, but for E+A galaxies.

6 EPS models. In each panel, the horizontal axis represents the 6 EPS models, and the vertical axis represents the contributed light fractions. The solid lines connect the resulted light fractions corresponding to group No. (1). The dotted, dashed, and long dashed lines indicate the relations between the light fractions inferred for the SSP groups Nos. (2), (3), and (4), respectively.

In these comparisons, we generally find that adding more SSPs within each age bin (based on the "standard case") results in more young populations (see the top-left panel), but removing SSPs does not result in consistent trend for them. In each EPS model, most of the changes in young populations (top-left panel) are ∼1–10% among different SSP groups. The biggest changes occur between the groups Nos. (1) and (4) in CB07 (∼16%) as well as between groups Nos. (2) and (4) in GALEV (∼15%). Adding or removing SSPs results in fewer contributions from intermediate-age populations (the top-middle panel). The most obvious changes occur between the groups Nos. (1) and (4) in CB07 (∼20%) and between Nos. (2) and (3) in Ma05 (∼14%). The changes in old populations (the top-right panel) are related to the young and intermediate ones, since the sum of these three populations is equal to 100%.

We plot the corresponding results for E+A galaxies in the top panels of Fig. 4 to check the age dependences. The symbols and lines have the same meanings as in Fig. 3. It confirms the general trend in star-forming galaxies, i.e., adding more SSPs increases the young populations and decreases the intermediate populations, and 3 SSPs produce complex changes in the different models. The top-left panel shows that within each EPS model, most of the changes in young populations are around 0–5% among different SSP groups. The biggest ones occur between groups Nos. (1) and (4) in Ma05 as well as between groups Nos. (2) and (3) in GALEV (∼20%); the changes in intermediate-age and old populations are obvious in CB07 and Ma05, up to ∼18% and ∼25%. The reason could be that CB07 and Ma05 include the TP-AGB contributions when building their SSPs, and the E+A galaxies are dominated by intermediate-age populations, which are related to the TP-AGB stars. This could also explain the most obvious discrepancies in the intermediate-age populations of star-forming galaxies with different models (see top-middle panel of Fig. 3). Moreover, the obvious discrepancy of group No. (2) with 3 SSPs from others may mean that 3 SSPs are an insufficient number for this stellar population analysis of galaxies.

In summary, from the top panels in Figs. 3 and 4, we can comment that the SSPs with different sets of ages obviously present different results (such as CB07, Ma05), although the discrepancies from both the models and ages will not change the dominant population of the galaxies.

4.4.2. Metallicity dependences – SSP groups Nos. (5)–(9) in Table 3

We fix the selections of age as the same as in the group No. (1) (Table 3, solar metallicity), then we add sub-solar metallicity or/and super-solar metallicity to construct groups Nos. (5)–(7) (Table 3). By comparing the results from these SSP groups with those from group No. (1), we can check the metallicity effects on spectral synthesis results.

The middle panels in Fig. 3 show the light fraction contributions from young (middle-left panel), intermediate (middle-middle panel), and old (middle-right panel) populations to star-forming galaxies by using the 6 EPS models. The solid lines connect the resultant light fractions corresponding to group No. (1) from different EPS models. The dotted, short dashed, and long dashed lines refer to the connections of the light fractions inferred by the SSP groups Nos. (5), (6), and (7), respectively.

These results show that within each EPS model all of the changes in young populations are smaller than 5%. The changes in intermediate-age populations (middle-middle panel) are larger and are in a range of 0–17%, such as ∼17% between groups Nos. (5) and (6) in CB07, and ∼13% between groups Nos. (5) and (6) in Ma05. For the old population (middle-right panel), the changes are also obvious among these SSP groups (0–17%), e.g., ∼14% between groups Nos. (5) and (6) in CB07, ∼17% between groups Nos. (5) and (6) in GALEV. The more obvious changes in CB07 and Ma05 may be related to the involved TP-AGB stars in their SSPs.

We present the corresponding results for E+A galaxies in the middle panels in Fig. 4. This shows that within each EPS model, all changes in young populations are not obvious (smaller than 6%); In general the changes in intermediate-age populations and old populations are also not obvious except for CB07. The differences are about 15% between groups Nos. (5) and (6) in intermediate population, and about 15% between groups Nos. (5) and (7) (as well as (6)) in old population (within CB07). These could also be due to the TP-AGB effect.

From the middle panels in Figs. 3 and 4, we deduce that SSPs with different selections of metallicities give different results.

By comparing the top panels with the middle panels in Figs. 3 and 4, We can see that the effects of metallicity are smaller than those of age. However, this phenomenon may be due to either the way we show our results or the age-metallicity degeneracy. We note that up to now, we have focused on the contributions of light fractions, whereas other properties, such as M/L, may be sensitive to metallicity. Maraston (2005) illustrated some parameters' dependences on metallicity, for example: the IR indices C_2 in their Fig. 16, the M^*/L in their Fig. 23, the D_{4000} in their Fig. 25, and the indices CaT^*, CaT and PaT in their Fig. 26. Longhetti & Saracco (2009) also presented the M/L as a function of metallicity in their Figs. 3–5.

We also note that the age-metallicity degeneracy may affect our adding or removing SSPs in the top and middle panels in Figs. 3 and 4. For this reason, we constructed the last two SSP groups, in which we changed only the metallicities and fixed all the ages. We present the results of these two groups in the bottom three panels of Figs. 3 and 4. From the bottom three panels, we see a much larger scatter (up to 40%) among different SSP groups than in the middle panels, implying that an age-metallicity degeneracy affects our Figs. 3 and 4. In our current paper, we do not study any further this classic degeneracy between age and metallicity, and some related studies can be found in Cid Fernandes et al. (2005), Eminian et al. (2008), Carter et al. (2009), and Cid Fernandes & González Delgado (2009).

Table 5. Stellar populations in each galaxy type by using six SSPs (group No. (1)) in different cases of tracks and libraries.

Galaxy types	Age bin	BC03 Pa94	BC03 Pa00	GALEV Pa94	GALEV Geneva	BaSeL3.1
star-forming	Y	35	31	47	41	49
	I	54	51	39	48	40
	O	11	18	14	11	11
composite	Y	31	29	42	39	40
	I	53	50	39	47	42
	O	16	21	19	14	17
E+A	Y	13	9	22	20	19
	I	77	71	71	72	72
	O	10	20	7	8	9
Seyfert 2	Y	6	10	2	0	0
	I	32	23	34	30	29
	O	35	42	26	31	29
	PL	27	25	38	39	42
LINER	Y	0	3	0	0	0
	I	24	16	26	22	20
	O	58	65	50	58	54
	PL	18	16	24	20	26
early type	Y	6	7	0	0	0
	I	7	2	40	20	31
	O	87	91	60	80	69

Notes. PL represents power law.

5. Dependences on evolution track, stellar spectral library, and the age sequence of galaxies

We check in greater detail the effects of stellar evolution tracks on the stellar population analysis of galaxies. We consider only the BC03 and GALEV models in this check. We use these two models to analyze the stellar populations of all the six representative samples of galaxies, i.e., the star-forming, composite galaxies, Seyfert 2s, LINERs, E+A and early-type galaxies, and compare the different properties of the stellar populations of each galaxy type.

5.1. Dependences on stellar evolution track and stellar spectral library

We use SSP group No. (1) (in Table 3) with Salpeter IMF, and with two different sets of stellar evolution tracks (Pa94 and Pa00 in BC03; Pa99 and Geneva in GALEV). The contributed light fractions of young, intermediate, and old populations are listed in Table 5. The first two columns corresponding to BC03 indicate that within each galaxy type, among different choices of stellar evolution tracks, the corresponding changes in young populations are 0–4%, in intermediate populations are 0–9%, and in old populations are 0–10%. While most of the results for GALEV (last two columns) are similar to BC03, except for the changes in intermediate and old populations of early-type galaxies (20%). These results imply that altering stellar evolution track will not significantly change the implied stellar populations of all the six types of galaxies.

We also mentioned in Sect. 4.3.1 that different selections of libraries may be another factor affecting our results. We therefore compared the two different libraries provided by BC03 (Table 5). One library is STELIB and the other is BaSeL3.1, and we fixed the IMF to be Salpeter and the track to be Pa94. We find that the results for BaSeL3.1 differ from those for STELIB, but the results of BaSeL3.1 are similar to those of GRASIL and GALEV. This supports our previous discussions in Sect. 4.3.1.

Gonzalez Delgado & Cid Fernandes (2009) also commented that the STELIB-based models produced metallicities of the star clusters systematically smaller by about 0.6 dex with respect to that was found with other models, but ages were probably right. The fact was that STELIB significantly underestimated metallicities with respect to both the CaII triplet and the metallicities from Leonardi & Rose (2003). A similar conclusion was derived by Koleva et al. (2008) in their analysis of Galactic globular clusters.

5.2. The age sequence

Since all the six types of sample galaxies are studied on their stellar populations, we can further study whether there is any age sequence among them. This could be an extended study of Chen et al. (2009), in which we have shown that there is an age sequence from star-forming galaxies, through composite galaxies, Seyfert 2s to LINERs, since the young populations decrease following this sequence.

In addition to the information about the dependences of our spectral synthesis model results on stellar evolution track, the numbers in Table 5 also indicate a possible age sequence among six different galaxy types. In our earlier work, we suggested that there was an age sequence from star-forming, composite galaxies, Seyfert 2s, to LINERs. Here we confirm these results and also consider E+A and early-type galaxies. It implies that the young populations diminish in significance from star-forming and composite galaxies, through E+A galaxies, Seyfert 2s, and LINERs, to early-type galaxies. In addition, E+A galaxies are dominated by intermediate-age populations. Early-type galaxies are certainly the oldest of all galaxy types. We therefore conclude there is a possible age sequence from star-forming, composite galaxies, through E+A galaxies, Seyfert 2s, and LINERs to early-type galaxies. A similar conclusion was reached by Schawinski et al. (2007), who identified an evolutionary sequence from star formation through nuclear activity to quiescence, i.e., from star-forming galaxies through transition region (similar to the composite galaxies in our sample) and Seyfert AGN and LINER galaxies to quiescence. This is also consistent with the results of both Cid Fernandes et al. (2009b) and Stasinska (2008).

6. Conclusion

We have compared 6 popularly used EPS models BC03, CB07, Ma05, GALEV, GRASIL, and Vazdekis/Miles. We have adopted the SSPs that they provide to fit the full spectral range of optical spectra of six representative types of galaxies (star-forming and composite galaxies, Seyfert 2s, LINERs, E+A, and early-type galaxies), which were taken from SDSS. We have investigated in detail the dependences of stellar population synthesis on EPS model, age, metallicity, and stellar evolution track. We have also studied the age sequence of these different types of galaxies. Our main results are:

1. The spectral fits that we have achieved for various galaxies using different EPS models are excellent except possibly for problematic regions, such as the area around H_β line in a few cases.
2. We have selected 6 SSPs of fixed age, metallicity, IMF and stellar evolution track from each EPS model to fit the spectra of star-forming and E+A galaxies to explore the dependence of the inferred stellar population properties on EPS models. We remark that it is a complex remains a difficult task to analyze the stellar populations of galaxies, different EPS models providing quite different results (such as BC03 vs. Vazdekis/Miles).
3. We have fixed the IMF, metallicity, and stellar evolution track, and varied the age to construct different SSP groups from the 6 EPS models, and then fitted the spectra of star-forming and E+A galaxies. Thus we have been able to study how the accuracy of stellar population synthesis models depends on age. Our results demonstrate that the stellar population synthesis does depend on how the ages are selected.
4. We then fixed the IMF, age, and stellar evolution tracks, and change the selection of metallicities to construct more different SSP groups from the 6 EPS models. We then fitted the spectra of star-forming and E+A galaxies, to study the dependence of stellar population synthesis on metallicities, our results indicating that there is a dependence on metallicity which is weaker than on ages. We note that this weaker dependence on metallicity than age may be due to either the way we have presented our results or the classic age-metallicity degeneracy.
5. Next we fixed the age and metallicity and changed the selection of stellar evolution tracks in BC03 and GALEV models, respectively. We then used them to fit the spectra of 6 galaxy types to determine the effect of stellar evolution track on the stellar population synthesis results. The results show that the stellar evolution track does not have a significant effect on the stellar population synthesis.
6. We also compared the stellar population synthesis results for different types of galaxies, and identified a possible age sequence: the importance of young populations decreases from star-forming, composite, Seyfert 2, LINER to early-type galaxies, and the importance of young populations of E+A galaxies lie between composite galaxies and Seyfert 2s in most cases.

Acknowledgements. We thank our referee for the valuable comments and suggestions, which helped improve this work. We thank Stephane Charlot and Gustavo Bruzual for kindly sending us the new version of their CB07 model, also thank Jingkun Zhao for doing de-resolution for our spectra. X. Y. Chen also thanks Yue Wu for helpful discussions on using ULySS. We thank the NSFC grant support under Nos. 10933001, 10973006, 10973015, 10673002, and the National Basic Research Program of China (973 Program) Nos. 2007CB815404, 2007CB815406, and No. 2006AA01A120 (863 project).
Funding for the SDSS and SDSS-II has been provided by the Alfred P. Sloan Foundation, the Participating Institutions, the National Science Foundation, the US Department of Energy, the National Aeronautics and Space Administration, the Japanese Monbukagakusho, the Max Planck Society, and the Higher Education Funding Council for England. The SDSS Web Site is http://www.sdss.org/.
The SDSS is managed by the Astrophysical Research Consortium for the Participating Institutions. The Participating Institutions are the American Museum of Natural History, Astrophysical Institute Potsdam, University of Basel, University of Cambridge, Case Western Reserve University, University of Chicago, Drexel University, Fermilab, the Institute for Advanced Study, the Japan Participation Group, Johns Hopkins University, the Joint Institute for Nuclear Astrophysics, the Kavli Institute for Particle Astrophysics and Cosmology, the Korean Scientist Group, the Chinese Academy of Sciences (LAMOST), Los Alamos National Laboratory, the Max-Planck-Institute for Astronomy (MPIA), the Max-Planck-Institute for Astrophysics (MPA), New Mexico State University, Ohio State University, University of Pittsburgh, University of Portsmouth, Princeton University, the United States Naval Observatory, and the University of Washington.

References

Alongi, M., Bertelli, G., Bressan, A., et al. 1993, A&AS, 97, 851
Anders, P., & Alvensleben, U. Fritze-v. 2003, A&A, 401, 1063
Asari, N. V., Cid Fernandes, R., Stasińska, G., et al. 2007, MNRAS, 381, 263

Asari, N. V., Stasińska, G., Cid Fernandes, R., et al. 2009, ASPC, 408, 176
Baldwin, J. A., Phillips, M. M., & Terlevich, R. 1981, PASP, 93, 5
Bertelli, G., Bressan, A., Chiosi, C., Fagotto, F., & Nasi, E. 1994, A&A, 106, 275
Bica, E. 1988, A&A, 195, 76
Boisson, C., Joly, M., Moultaka, J., Pelat, D., & Roos, M. S. 2000, A&A, 357, 850
Bressan, A., Fagotto, F., Bertelli, G., & Chiosi, C. 1993, A&AS, 100, 647
Brinchmann, J., Charlot, S., White, S. D. M., et al. 2004, MNRAS, 351, 1151
Bruzual, A. G. 1983, ApJ, 273, 105
Bruzual, A. G. 2005, [arXiv:astro-ph/0701907]
Bruzual, A. G., & Charlot, S. 1993, ApJ, 405, 538
Bruzual, A. G., & Charlot, S. 2003, MNRAS, 344, 1000
Calzetti, D., Kinney, A. L., & Storchi-Bergmann, T. 1994, ApJ, 429, 582
Carter, D., Smith, D. J. B., Percival, S. M., et al. 2009, MNRAS, 397, 695
Cassisi, S., Castellani, M., & Castellani, V. 1997a, A&A, 317, 108
Cassisi, S., Degl'Innocenti, S., & Salaris, M. 1997b, MNRAS, 290, 515
Cassisi, S., Castellani, V., Ciarcielluti, P., Piotto, G., & Zoccali, M. 2000, MNRAS, 315, 679
Cenarro, A. J., Cardiel, N., Gorgas, J., et al. 2001, MNRAS, 326, 959
Chabrier, G. 2003, PASP, 115, 763
Chen, X. Y., Hao, C. N., & Wang, J. 2008, Chinese J. Astron. Astrophys., 8, 25
Chen, X. Y., Liang, Y. C., Hammer, F., Zhao, Y. H., & Zhong, G. H. 2009, A&A, 495, 457
Cid Fernandes, R., & González, D., 2010 MNRAS, 403, 780
Cid Fernandes, R., Sodré, L., Schmitt, H. R., & Leão, J. R. S. 2001, MNRAS, 325, 60
Cid Fernandes, R., Gu, Q., Melnick, J., et al. 2004, MNRAS, 355, 273
Cid Fernandes, R., Mateus, A., Sodré, L., Stasińska, G., & Gomes, J. M. 2005, MNRAS, 358, 363
Cid Fernandes, R., Asari, N. V., Sodré, L., et al. 2007, MNRAS, 375, 16
Cid Fernandes, R., Schlickmann, M., Stasinska, G., et al. 2009a, The Starburst-AGN Connection, ed. W. M. Wang, Z. Q. Yang, Z. J. Luo, & Z. Chen, ASP Conf. Ser., 408, 122
Cid Fernandes, R., Schoenell, W., Gomes, J. M., et al. 2009b, RMxAC, 35, 127
Coelho, P. 2009, Probing Stellar Populations out to the Distant Universe: CEFALU 2008, AIP Conf. Proc., 1111, 67
Conroy, C., & Gunn, J. E. 2010, ApJ, 712, 833
Conroy, C., Gunn, J. E., & White, M. 2009, ApJ, 699, 486
Conroy, C., White, M., & Gunn, J. E. 2010, ApJ, 708, 58
Cordier, D., Pietrinferni, A., Cassisi, S., & Salaris, M. 2007, AJ, 133, 468
Eggen, O. J., Lynden-Bell, D., & Sandage, A. R., 1962, ApJ, 136, 748
Eminian, C., Kauffmann, G., Charlot, S., et al. 2008, MNRAS, 384, 930
Faber, S. M. 1972, A&A, 20, 361
Fagotto, F., Bressan, A., Bertelli, G., & Chiosi, C. 1994a, A&AS, 104, 365
Fagotto, F., Bressan, A., Bertelli, G., & Chiosi, C. 1994b, A&AS, 105, 29
Falkenberg, M. A., & Fritze, U. 2009a, MNRAS, 397, 1940
Falkenberg, M. A., Kotulla, R., & Fritze, U., 2009b, MNRAS, 397, 1954
Fioc, M., & Rocca-Volmerange, B. 1997, A&A, 326, 950
Girardi, L., Bressan, A., Chiosi, C., Bertelli, G., & Nasi, E. 1996, A&AS, 117, 113
Girardi, L., Bressan, A., Bertelli, G., & Chiosi, C. 2000, A&AS, 141, 371
Goto, T. 2007, MNRAS, 381, 187
González Delgado, R. M., & Cid Fernandes, R. 2010, MNRAS, 403, 797
Hammer, F., Flores, H., Elbaz, D., et al. 2005, A&A, 430, 115
Hammer, F., Puech, M., Chemin, L., Flores, H., & Lehnert, M. D. 2007, ApJ, 662, 322
Hammer, F., Flores, H., Puech, M., et al. 2009, A&A, 507, 1313
Hao, C. N., Mao, S. D., Deng, Z. G., Xia, X. Y., & Wu H. 2006, MNRAS, 370, 1339
Heavens, A., Panter, B., Jimenez, R., & Dunlop, J. S. 2004, Nature, 428, 625
Hempel, M., Geisler, D., Hoard, D. W., & Harris, W. E. 2005, A&A, 439, 59
Huang, S., & Gu, Q. S. 2009, MNRAS, 398, 1651
Jehin, E., Bagnulo, S., Melo, C., Ledoux, C., & Cabanac, R., in The UVES Paranal Observatory Project: a public library of high resolution stellar spectra, ed. V. Hill, P. Francois, F., Primas 2005, IAU Symp., 261
Jimenez, R., MacDonald J., Dunlop, J. S., Padoan, P., & Peacock, J. A. 2004, MNRAS, 349, 240
Kauffmann, G., Heckman, T. M., Tremonti, C., et al. 2003, MNRAS, 346, 1055
Kennicutt, R. C. 1983, ApJ, 272, 54
Kennicutt, R. C. 1998, ARA&A, 36, 189
Kewley, L. J., Dopita, M. A., Sutherland, R. S., Heisler, C. A., & Tervena, J. 2001, ApJ, 556, 121
Kewley, L. J., Groves, B., Kauffmann, G., & Heckman, T. 2006, MNRAS, 372, 961
Koleva, M., Prugniel, Ph., Ocvirk, P., Le Borgne, D., & Soubiran, C. 2008, MNRAS, 385, 1998
Koleva, M., De Rijcke, S., Prugniel, Ph., Zeilinger, W. W., & Michielsen, D. 2009a, MNRAS, 396, 2133
Koleva, M., Prugniel, Ph., Bouchard, A., & Wu, Y. 2009b, A&A, 501, 1269
Koski, A. T. 1978, ApJ, 223, 56
Kotulla, R., Fritze, U., Weilbacher, P., et al. 2009, MNRAS, 396, 462
Kriek, M., van Dokkum, P. G., Franx, M., et al. 2006, ApJ, 645, 44
Kriek, M., van Dokkum, P. G., Franx, M., et al. 2007, ApJ, 669, 776
Kriek, M., van Dokkum, P. G., Franx, M., et al. 2008, ApJ, 677, 219
Kroupa, P. 2001, MNRAS, 322, 231
Kurucz R. L. 1992, in The Stellar Populations of Galaxies, ed. B. Barbuy, & A. Renzini, IAU Symp., 149, 225
Le Borgne, J.-F., Bruzual, G., Pelló, R., et al. 2003, A&A, 402, 433
Le Borgne, D., Rocca-Volmerange, B., Prugniel, P., et al. 2004, A&A, 425, 881
Lee, H.-C., Worthey, G., Trager, S. C., & Faber, S. M. 2007, ApJ, 664, 215
Leitherer, C., & Heckman, T. M. 1995, ApJS, 96, 9
Lejeune, Th., Cuisinier, F., & Buser, R. 1997, A&AS, 125, 229
Lejeune, Th., Cuisinier, F., & Buser, R. 1998, A&AS, 130, 65
Leonardi, A. J., & Rose, J. 2003, ApJ, 126, 1811
Longhetti, M., & Saracco, P. 2009, MNRAS, 394, 774
Maraston, C. 1998, MNRAS, 300, 872
Maraston, C. 2005, MNRAS, 362, 799
Maraston, C., Daddi, E., Renzini, A., et al. 2006, ApJ, 652, 85
Marigo, P., & Girardi, L. 2007, A&A, 469, 239
Mateus, A., Sodré, L., Cid Fernandes, R., et al. 2006, MNRAS, 370, 721
Mathis, H., Charlot, S., & Brinchmann, J., 2006, MNRAS, 365, 385
Miller, G. E., & Scalo, J. M. 1979, ApJS, 41, 513
Muzzin, A., Marchesini, D., & van Dokkum, P. G. 2009, ApJ, 701, 1839
Panter, B., Jimenez, R., Heavens, A. F., & Charlot, S. 2007, MNRAS, 378, 1550
Panter, B., Jimenez, R., Heavens, A. F., & Charlot, S. 2008, MNRAS, 391, 1117
Pessev, P., M., Goudfrooij, P., Puzia, T. H., & Chandar, R. 2008, MNRAS, 385, 1535
Pickles, A. J. 1998, PASP, 110, 863
Pietrinferni, A., Cassisi, S., Salaris, M., & Castelli, F. 2004, ApJ, 612, 168
Pracy, M. B., Kuntschner, H., Couch, W. J., et al., 2009, MNRAS, 396, 1349
Prugniel, P., Soubiran, C., Koleva, M., & Le Borgne, D. 2007, [arXiv:astro-ph/0703658], ELODIE Library, v.31
Raimondo, G., Brocato, E., Cantiello, M., & Capaccioli, M. 2005, AJ, 130, 2625
Salpeter, E. E. 1955, ApJ, 121, 161
Sánchez-Blázquez, P., Peletier, R. F., Jiménez-Vicente, J., et al. 2006, MNRAS, 371, 703
Scalo, J. 1998, in The Stellar Initial Mass Function, 38th, Herstmonceux Conference, ed. G., Gilmore, & D., Howell, ASP Conf. Ser., 142, 201
Schaller, G., Schaerer, D., Meynet, G., & Maeder, A. 1992, A&AS, 96, 269
Schawinski, K., Thomas, D., Sarzi, M., et al. 2007, MNRAS, 382, 1415
Schulz, J., Alvensleben, U., Fritze-v., Möller, C. S., & Fricke, K. J. 2002, A&A, 392, 1
Shuder, J. M., & Osterbrock, D. E. 1981, ApJ, 250, 55
Silva, L., Granato, G. L., Bressan, A., & Danese, L. 1998, ApJ, 509, 103
Stasińska, G., Asari, V. N., Cid Fernandes, R., et al. 2008, MNRAS, 391, 29
Stoughon, C., Lupton, R. H., Bernardi, M., et al. 2002, AJ, 123, 485
Tinsley, B. M. 1978, ApJ, 222, 14
Tremonti, C. A., Heckman, T. M., Kauffmann, G., et al. 2004, ApJ, 613, 898
Valdes, F., Gupta, R., Singh, H. P., & Bell, D. J. 2004, ApJS, 152, 251
Vazdekis, A. 1999, ApJ, 513, 224
Vazdekis, A., & Arimoto, N. 1999, ApJ, 525, 144
Vazdekis, A., Casuso, E., Peletier, R. F., & Beckman, J. E., et al. 1996, ApJS, 106, 307
Vazdekis, A., Cenarro, A. J., Gorgas, J., Cardiel, N., & Peletier, R. F., et al. 2003, MNRAS, 340, 1317
Vázquez, G. A., & Leitherer, C. 2005, ApJ, 621, 695
Veilleux, S., & Osterbrock, D. E. 1987, ApJS, 63, 295
Westera, P., Lejeune, T., Buser, R., Cuisinier, F., & Bruzual, G. 2002, A&A, 381, 524
White, S. D. M. 1984, ApJ, 286, 38
Worthey, G. 1994, ApJS, 94, 687